Radiocarbon, Vol 66, Nr 6, 2024, p 1898–1913 DOI:10.1017/RDC.2024.38
Selected Papers from the 24th Radiocarbon and 10th Radiocarbon & Archaeology International Conferences, Zurich, Switzerland, 11–16 Sept. 2022

ORIGIN AND AGE OF CARBON IN THE CELLULOSE OF MID-LATITUDE TREE RINGS

Bernd Kromer[1]* • Lukas Wacker[2]* • Michael Friedrich[3] • Susanne Lindauer[4] • Ronny Friedrich[4] • Julia Bitterli[2] • Kerstin Treydte[5,6] • Patrick Fonti[5,6] • Elisabet Martínez-Sancho[5,7] • Daniel Nievergelt[5]

[1]Institute of Environmental Physics, Heidelberg University, Germany
[2]Laboratory of Ion Beam Physics, ETH Zurich, Switzerland
[3]Hohenheim Gardens, University of Hohenheim, Stuttgart, Germany
[4]Curt-Engelhorn-Centre Archaeometry, Mannheim, Germany
[5]Research Unit Forest Dynamics, Swiss Federal Institute for Forest, Snow and Landscape Research WSL, Birmensdorf, Switzerland
[6]Oeschger Centre for Climate Change Research, University of Bern, Hochschulstrasse 4, CH-3012 Bern, Switzerland
[7]Department of Biological Evolution, Ecology and Environmental Sciences, University of Barcelona, 08028 Barcelona, Spain

ABSTRACT. Cellulose of tree rings is often assumed to be predominantly formed by direct assimilation of CO_2 by photosynthesis and consequently can be used to reconstruct past atmospheric ^{14}C concentrations at annual resolution. Yet little is known about the extent and the age of stored carbon from previous years used in addition to the direct assimilation in tree rings. Here, we studied ^{14}C in earlywood and latewood cellulose of four different species (oak, pine, larch and spruce), which are commonly used for radiocarbon calibration and dating. These trees were still growing during the radiocarbon bomb peak period (1958–1972). We compared cellulose ^{14}C measured in tree-ring subdivisions with the atmospheric ^{14}C corresponding to the time of ring formation. We observed that cellulose ^{14}C carried up to about 50% of the atmospheric ^{14}C signal from the previous 1–2 years only in the earlywood of oak, whereas in conifers it was up to 20% in the earlywood and in the case of spruce also in the latewood. The bias in using the full ring of trees growing in a temperate oceanic climate to estimate atmospheric ^{14}C concentration might be minimal considering that earlywood has a low mass contribution and that the variability in atmospheric ^{14}C over a few years is usually less than 3‰.

KEYWORDS: annual resolution, cellulose, non-structural carbon, radiocarbon, tree ring.

INTRODUCTION

Tree rings play a fundamental role in radiocarbon dating. Due to their absolute dating and annual resolution, tree rings provide a continuous radiocarbon reference for dating any carbonaceous sample of organic origin over the last ca. 14,000 years (Reimer et al. 2020). Recent technological improvements in radiocarbon measurements are now allowing sub-ring resolution (Xu et al. 2015; Cain et al. 2018; Kudsk et al. 2018; Turney et al. 2018; Svarva et al. 2019; McDonald et al. 2019) opening new opportunities for intra-annual dating. For such an application, questions regarding sub-ring radiocarbon variation and its variability across sites and species need to be clarified and understood.

Annual rings of most trees in the middle and high latitudes are composed of two parts, the earlywood (EW), formed at the beginning of the growing season, and the latewood (LW), whose formation begins in the summer. Moreover, since these two parts have multiple functions (water transport vs structural support) and display different cell anatomical

*Corresponding authors. Bernd Kromer; Email: bernd.kromer@iup.uni-heidelberg.de; Lukas Wacker; Email: wacker@phys.ethz.ch

characteristics, they also undergo cell formation processes with different timing, rates and requirements (Rathgeber et al. 2016, Rathgeber et al. 2022) that vary among species (Chen et al. 2022) and environments (Rossi et al. 2016). Phenological studies showed that in ring-porous deciduous species (e.g., oak) and deciduous conifers (e.g., larch) the process of earlywood formation starts around bud-burst time (e.g., Moser et al. 2009; Dox et al. 2022), i.e., when photosynthesis is still low and new assimilates for structural use are not yet available. This initial growth is mainly sustained by large pools of nonstructural carbohydrates (NSC), which are stored in the perennial tissues of trees and can be mobilized through the parenchyma/medullary rays. Medullary rays extend over many annual rings into the center of the tree and, in contrast to these, are alive over many years. A considerable part of the mobilizable NSC (especially starch) is deposited in these cells during the winter dormant period. However, these pools are a mixture of NSC with different ages (see Gessler and Treydte 2016). The contribution of reserves accumulated from the previous year or years to initial growth has been also supported by studies using tree-ring stable isotopic information (Helle and Schleser 2004; Gessler and Treydte 2016; Boettger and Friedrich 2009). The latewood, on the other hand, begins formation in the summer, when the leaves/needles are fully functional. Thus, growth and metabolic activity are mainly maintained by recent assimilates, although there are still some uncertainties about how this pattern is modified under stressful conditions such as extreme droughts.

This mix of ^{14}C signatures from old and new assimilates within a single tree-ring naturally raises the question of the extent to which the carbon of an annual ring matches the atmospheric ^{14}C concentration of the year or more precisely the season of growth. This consideration has large relevance nowadays, as ^{14}C is now more easily measured even at intra-ring resolution. The strongest observed intra- and interannual atmospheric ^{14}C fluctuations occurred during the atmospheric bomb testing period between 1955 and 1962, and the successive decline in atmospheric ^{14}C. This period provides an ideal framework to tackle questions regarding the amount of incorporation of previous years carbon in a tree-ring in addition to the direct uptake from the atmosphere.

Several studies have used the bomb-spike period to investigate the age of the atmospheric ^{14}C uptake in tree rings. Grootes et al. (1989) studied the 1962–1964 tree rings in spruce from the US Pacific coast and concluded "that there is little or no contribution of stored photosynthate to radial growth." Olsson and Possnert (1992) observed that earlywood ^{14}C concentration of Swedish oak was clearly lower than the atmospheric values for 1962 and 1963 indicating significant use of stored carbon from previous years. In a more recent study by (Kudsk et al. 2018), no influence of stored carbon was found in either earlywood or latewood in Danish oak by measuring the ^{14}C content of the cellulose for the years 1954–1970.

MATERIAL AND METHODS

Sample Selection

For our study, we selected a deciduous ring-porous species (oak), a deciduous coniferous larch, and two evergreen coniferous species with different needle retention times (5–7 years for spruce, 4–5 years for pine). For each species, we analyzed one individual. In addition, we compared lowland to highland trees, the latter of which have a shorter growing season (Figure 1). The selected species are among the most commonly used for the development of the radiocarbon calibration data sets (Stuiver et al. 1986; Reimer et al. 2004; Bayliss et al. 2020):

https://doi.org/10.1017/RDC.2024.38 Published online by Cambridge University Press

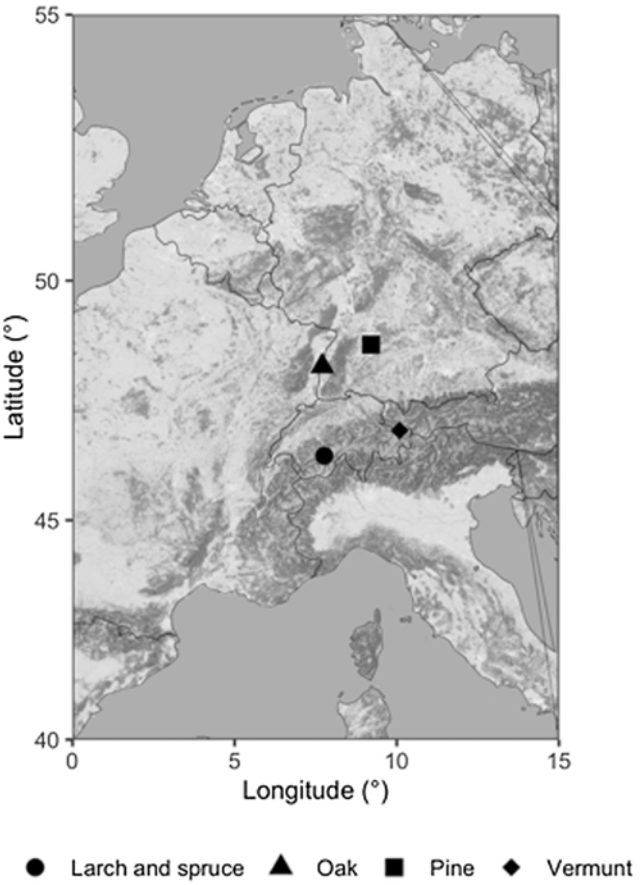

Figure 1 Geographic locations of the sites of the four species (one tree each) selected in this study, and of the Central European ^{14}C background site in Vermunt, Austria.

(1) Oak (*Quercus robur* L.) from Rust in the Upper Rhine valley, Germany (48°16'04,6''N; 7° 42'09,5''E; 160 m a.s.l.) – ring-porous deciduous tree species.

(2) Pine (*Pinus nigra* Arnold) from Botanical Garden at Stuttgart-Hohenheim, Germany (48° 42'37,8''N; 9°12'25,4''E; 380 m a.s.l.) – evergreen conifer

(3) Larch (*Larix decidua* Mill.) from Lötschental, Switzerland, (46°23'30.42''N; 7°45'40.8''E; 1300 m a.s.l.) deciduous conifer, 1-year needles

(4) Spruce (*Picea abies* (L.) Karst.) from Lötschental, Switzerland (46°23'30.42''N; 7° 45'40.8''E; 1300 m a.s.l.) evergreen conifer

The oak from Rust was a healthy, ca. 130-year-old, living tree from a hardwood floodplain forest in the "Taubergiessen" nature reserve in the Upper Rhine valley. The oak was a predominant tree from the overstory with an exposed crown. The black pine comes from the Botanical Garden of the University of Hohenheim. Before it fell over in a storm, it was ca. 140-year-old and ca. 25-m-high solitary tree without any understory.

https://doi.org/10.1017/RDC.2024.38 Published online by Cambridge University Press

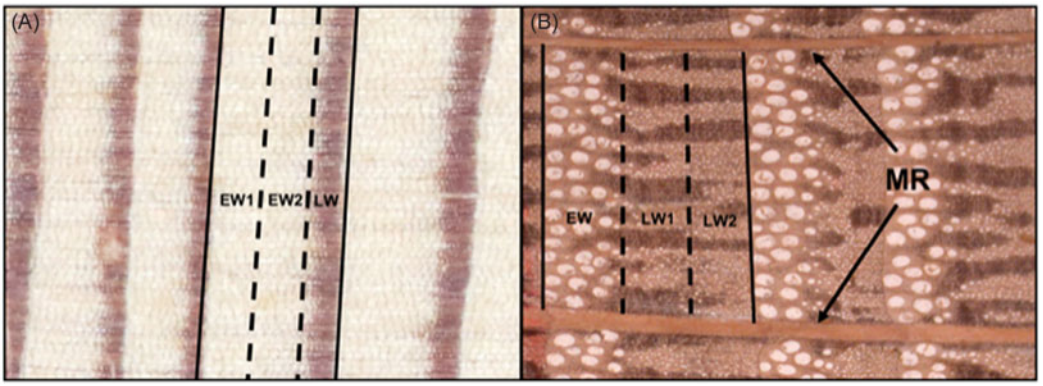

Figure 2 Scheme of sampling: A) Conifer (larch), B) oak. Due to the differences in the proportions of each whole ring represented by the earlywood and the latewood in conifers and oak, the earlywood (EW) in conifers has been divided into two sections (EW1, EW2) and latewood (LW) in one section. The oak tree rings were divided into one earlywood (EW) and two latewood (LW1, LW2) sections. In oak, the broad medullary rays (MR) are excluded for analysis.

We divided the individual tree rings into three subsections, which are supposed to represent three easily defined sections of the wood increment: Ring-porous deciduous tree species (oak): one section of earlywood (EW1), two sections of latewood (LW1, LW2). Conifer trees (pine, larch and spruce): Two sections of earlywood (EW1, EW2) and one section of latewood (LW) (Figure 2).

In addition to the longitudinally oriented wood cells, the annual rings of all wooden species are interspersed with radially oriented medullary rays, which extend over many annual rings into the center of the tree, and which are alive over many years (Gessler and Treydte 2016). Because of the extended life of these medullary ray cells and to avoid any possible contamination by translocation of older or younger carbon, we have removed the medullary rays in the oak annual rings as best we could by preparation. This is possible with oak wood because the medullary rays are present in a number of large bundles and can therefore be easily identified and removed under the light microscope. This is not feasible with conifer wood because the numerous medullary rays that are only a few cell rows wide are spread over the entire cross-section.

Growth periods

For pine and oak trees, we estimated the mean earlywood and latewood growth periods based on continuous dendrometric measurements at Hohenheim Botanical Garden in 1990's and 2000's aligned with leaf phenological observation data of the investigated tree species at sample sites Hohenheim and Rust, which cover the entire period of dendrometric measurement and leaf phenological observations (Holz et al. 2010). We took into account that in northern hemisphere conifers cell enlargement and wall thickening are completed several weeks earlier than lignification (subsequent incorporation of lignin into the cell walls made of cellulose), which continues into late autumn (Cuny et al. 2015). This is of particular interest here because we only measure ^{14}C in the cellulose, as is standard procedure for high-precision ^{14}C dating. For the larch and spruce trees from the Lötschental, we estimated the period of tracheid secondary wall deposition to EW1, EW2 and LW as the average of cellular observations (from

https://doi.org/10.1017/RDC.2024.38 Published online by Cambridge University Press

weekly microcores) performed for 4 trees per species at the same sites during the period 2008 to 2013.

The calculations have been performed according to the method described in Cuny et al. (2019) and Pérez-de-Lis et al. (2022). Primary data, namely repeated cellular observations performed on stem microcores, were obtained from Cuny et al. (2019). The cellular observations allowed determination of the time of tracheid enlargement and secondary wall deposition. Since cellulose deposition of the secondary wall includes most of the cellulose used in the ring structure, and since lignin deposition co-occurs with a temporal offset of few days (see Rathgeber et al. 2022), the timing of cellulose deposition and the observations of secondary wall deposition are given in Table 1. The phenology of the 2008-2013 observations were assumed to be an acceptable estimate for the phenology 1962-1965 since difference in the timing of peak climatic signal in wood cell anatomical features between early and late twentieth century have been shown to only have a minimal shift of a few days (Carrer et al. 2017).

Sample Preparation and AMS Measurement

All samples were pretreated for holocellulose using the BABAB technique (Němec et al. 2010). The pretreatment starts with a base step overnight at 60°C (4% NaOH), followed by an acid step using 2M HCl, an additional base step before the final acid step. In between each step the samples were always washed two to three times with ultrapure water.

Holocellulose was then extracted by using sodium chlorite, where hydrochloric acid (HCl) was added until pH 3. The NaClO2 solution was repeatedly replaced after 2 hours until the remaining holocellulose was white. Then the samples were washed twice with ultrapure water and dried before being combusted in an elemental analyzer (Microcube, elementar) and graphitized in an AGE III system (Ionplus) (Wacker et al. 2010). The oak and the pine samples were measured at the CEZA laboratory, Mannheim, Germany (sample identifier starting with "MAMS") (Kromer et al. 2013) while the spruce and larch samples were measured in ETH Zurich, Switzerland (Wacker et al. 2010). Blank measurements were done on phthalic anhydride as a measurement blank, but also on wood samples (process blanks) undergoing the same pretreatment together with the samples and containing no ^{14}C (lignite from Reichwalde in Germany and Kauri wood from New Zealand) (Sookdeo et al. 2020).

Time Series of the Central European Atmospheric ^{14}C Concentrations

Essential for this study is the ^{14}C concentration of continental background air in Central Europe during the interval of ring growth over the respective years. For the northern hemisphere monthly ^{14}C data were combined into a sector NH1 from atmospheric measurements from Norway, Austria (Vermunt) and China Lake (USA) (Hua et al. 2013) We decided to compare the tree-ring ^{14}C to only the ^{14}C measurements in the Austrian mountains (Vermunt, Montafon, Figure 1) for these reasons:

(1) Only in Vermunt did the ^{14}C measurements start by 1959, covering fully the interval of our samples (Levin et al. 1985), with several days of sampling at the center of each month of the year during the interval considered in this study.

(2) The Vermunt data could be compared to the 1966 to 1983 data of a site close to the oak site (50 km distance), Schauinsland at 1100 m asl above the Rhine valley, and close agreement has been found (Levin et al. 1985, Figure 2).

https://doi.org/10.1017/RDC.2024.38 Published online by Cambridge University Press

Table 1 Years of ^{14}C measurement and estimated growth periods for the subsections of the annual rings.

Species	Altitude asl (m)	Years of ^{14}C data	Start EW1/ EW	End EW1/ EW	Start EW2	End EW2	Start LW1/ LW	End LW1/ LW	Start LW2	End LW2
Oak Rhine Valley	160	1955-1973	Apr 15	May 30			May 20	July 10	July 1	Sep 16
Pine Stuttgart	380	1958-1972	March 29	May 12	May 5	June 30	June 20	Sep 15		
Larch	1300	1962-1965	June 17	July 24	July 2	Sep 09	July 6	Aug 19		
Spruce	1300	1962-1965	June 6	July 26	June 30	Sep 13	July 7	Sep 07		

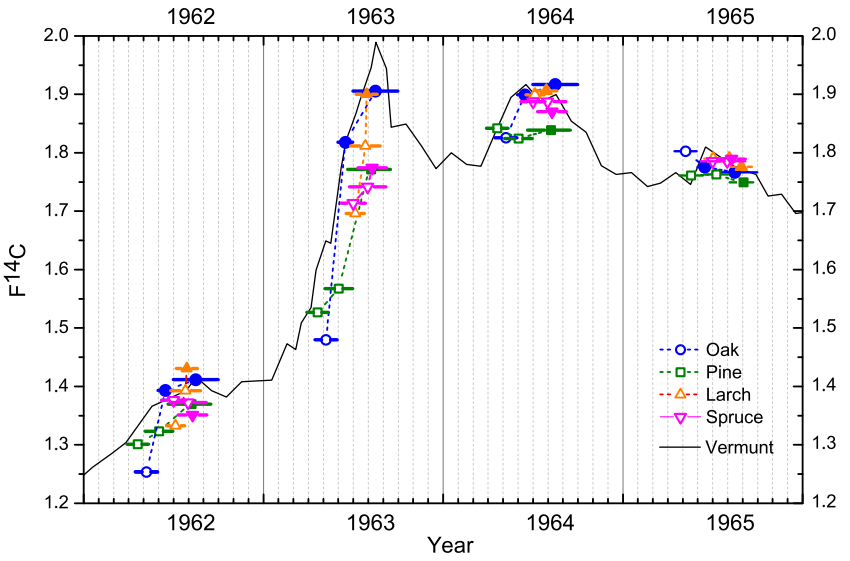

Figure 3 $F^{14}C$ of earlywood (open symbol) and latewood (filled symbol) of all four species in the interval of 1962–1965, compared to data of an atmospheric sampling site (Vermunt, Germany). Growth periods indicated by horizontal bars.

RESULTS

The data are shown in Figure 3 for the full set of the four species, and in Figure 4 for the extended interval of 1965 to 1972 for the oak and pine species. The full ^{14}C dataset of all species and ring sectors is given in the supplementary table.

We observed considerable differences between the species:

(1) $F^{14}C$ in latewood of oak agreed well with the Vermunt ^{14}C activity, but the earlywood was considerably lower in the years 1962 and 1963, and higher for 1965 and the following years. The EW fraction of the oak tree shows up to 11% lower values the biggest offsets compared to the atmosphere compared with all the other tree-ring fractions.

(2) $F^{14}C$ in earlywood and latewood of pine follow closely the transitions of Vermunt, but they are shifted significantly to lower values than Vermunt (mean difference 1959-1972 $\Delta F^{14}C$=0.025). The difference could come from lower $^{14}CO_2$ of soil carbon (heterotrophic respiration) or from fossil CO_2. Measured CO2 levels in Stuttgart-Hohenheim (near the airport Stuttgart and a major highway) in the year 2002 were 29 ppm higher compared to the natural reserve site in the Rhine valley, the location of the oak. Hence, depletion of the atmospheric ^{14}C content by fossil fuel CO2 is the plausible explanation, and it is corrected for in the model calculations of the section below. After correction, an insignificant contribution from NSC from previous years can be seen in the $F^{14}C$ signature of the earlywood as well of the latewood. Soil carbon has a longer average residence time, so we should observe low bomb test ^{14}C in this contribution before 1965, and higher ^{14}C than atmospheric ^{14}C later, which is not the case.

(3) The $F^{14}C$ in the deciduous larch follows more closely the atmospheric values of Vermunt in 1962 and 1963 than the deciduous oak tree, though here also the EW is a bit lower. In the following years 1964 and 1965 the $F^{14}C$ of EW follows closely the atmosphere.

https://doi.org/10.1017/RDC.2024.38 Published online by Cambridge University Press

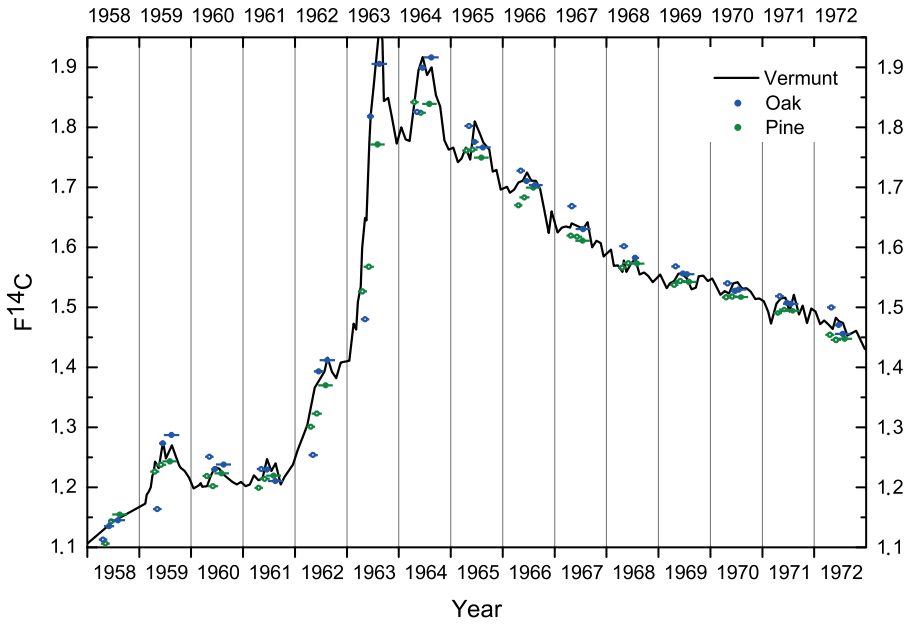

Figure 4 $F^{14}C$ in earlywood (open symbol) and latewood (filled symbols) of oak and pine (not corrected for fossil CO_2) in the interval 1958–1972.

(4) The $F^{14}C$ in the spruce in general, but more specifically in the latewood of 1962 and 1963, is significantly lower than Vermunt $F^{14}C$. At this site, fossil CO_2 influence can be excluded because of the Alpine clean air site and the correct larch latewood values from the same location, so the earlywood ^{14}C results can therefore be considered unbiased by fossil-fuel CO_2. While the $F^{14}C$ for 1964 is still a little bit lower, for 1965 it agrees well with the atmosphere.

Modeling

To better understand and interpret our obtained results, a simple model was applied to compare the measured ^{14}C content of the tree-ring sections with the theoretical ^{14}C concentration assuming direct assimilation of CO_2 by photosynthesis and continuous integration into the cellulose. For the model, we assumed the amount of woody biomass and thus also the cellulose production (Cuny 2015) to be gaussian shaped around mid-summer (July 7th). The width of the distribution was adjusted to the assumed growth period of the trees at the different locations, with a shorter period for the high-elevation trees from the Lötschental (full width at half maximum: 0.25 yr^{-1}) and a longer period for the low-elevation trees from Southern Germany (fwhm: 0.31 yr^{-1}).

We then calculated the theoretical radiocarbon concentration (atmospheric $F^{14}C$, Table 2) assuming the formed cellulose was based on the direct assimilation of atmospheric CO_2 and on a rapid transport from source to sink (Epron, 2012). This was done by integrating accordingly the interpolated atmospheric ^{14}C concentrations from Vermunt (Levin 1985) over the growth periods for the equivalent EW and LW fractions (see table 2, ring portion).

https://doi.org/10.1017/RDC.2024.38 Published online by Cambridge University Press

Table 2 Measured and modeled radiocarbon concentrations expected for direct atmospheric (Levin et al. 1985) uptake in the tree rings. Also shown are values for a storage pool with NSC reserves that can be remobilized and incorporated into the cellulose cell wall of current year, with a best-fit annual exchange rate to estimate the integration of pre-aged carbon in addition to direct uptake from the atmosphere.

	Year (CE)	Fraction	ring portion (g/g)	measured $F^{14}C$	atmosph. $F^{14}C$	difference meas.-atm.	NSC $F^{14}C$	fraction NSC	NSC exchange rate (yr^{-1})
Oak	1962	EW1	0.20	1.2539±0.0031	1.3665	−8%	1.2280	81%	70%
	1962	LW1	0.40	1.3934±0.0033	1.3965	0%	1.2280	2%	70%
	1962	LW2	0.40	1.4118±0.0033	1.4047	1%	1.2280	−4%	70%
	1963	EW1	0.20	1.4798±0.0024	1.6633	−11%	1.3439	57%	70%
	1963	LW1	0.40	1.8182±0.0022	1.8589	−2%	1.3439	8%	70%
	1963	LW2	0.40	1.9056±0.0022	1.9290	−1%	1.3439	4%	70%
	1964	EW1	0.20	1.8258±0.0040	1.8879	−3%	1.6966	32%	70%
	1964	LW1	0.40	1.8992±0.0042	1.9014	0%	1.6966	1%	70%
	1964	LW2	0.40	1.9168±0.0042	1.8728	2%	1.6966	−25%	70%
	1965	EW1	0.20	1.8026±0.0040	1.7723	2%	1.8296	53%	70%
	1965	LW1	0.40	1.7755±0.0039	1.7985	−1%	1.8296	−74%	70%
	1965	LW2	0.40	1.7664±0.0039	1.7686	0%	1.8296	−4%	70%
Pine (scaled 1.02)	1962	EW1	0.33	1.3269±0.0030	1.3752	−4%	1.2280	33%	70%
	1962	EW2	0.33	1.3495±0.0030	1.4027	−4%	1.2280	30%	70%
	1962	LW1	0.33	1.3972±0.0031	1.4034	0%	1.2280	4%	70%
	1963	EW1	0.33	1.5574±0.0029	1.7229	−10%	1.3439	44%	70%
	1963	EW2	0.33	1.5990±0.0030	1.8939	−16%	1.3439	54%	70%
	1963	LW1	0.33	1.8069±0.0032	1.9271	−6%	1.3439	21%	70%
	1964	EW1	0.33	1.8788±0.0034	1.8979	−1%	1.6966	10%	70%
	1964	EW2	0.33	1.8610±0.0034	1.8963	−2%	1.6966	18%	70%
	1964	LW1	0.33	1.8757±0.0033	1.8678	0%	1.6966	−5%	70%
	1965	EW1	0.33	1.7965±0.0044	1.7867	1%	1.8296	23%	70%
	1965	EW2	0.33	1.7980±0.0032	1.7916	0%	1.8296	17%	70%
	1965	LW1	0.33	1.7844±0.0033	1.7658	1%	1.8296	29%	70%

Table 2 (*Continued*)

	Year (CE)	Fraction	ring portion (g/g)	measured $F^{14}C$	atmosph. $F^{14}C$	difference meas.-atm.	NSC $F^{14}C$	fraction NSC	NSC exchange rate (yr^{-1})
Spruce	1962	EW1	0.33	1.3767±0.0021	1.3819	0%	1.2189	3%	50%
	1962	EW2	0.33	1.3724±0.0021	1.4027	−2%	1.2189	16%	50%
	1962	LW1	0.33	1.3511±0.0021	1.4063	−4%	1.2189	29%	50%
	1963	EW1	0.33	1.7138±0.0025	1.7599	−3%	1.3079	10%	50%
	1963	EW2	0.33	1.7419±0.0025	1.8931	−8%	1.3079	26%	50%
	1963	LW1	0.33	1.7743±0.0026	1.9437	−9%	1.3079	27%	50%
	1964	EW1	0.33	1.8874±0.0027	1.9048	−1%	1.5868	5%	50%
	1964	EW2	0.33	1.8876±0.0027	1.8951	0%	1.5868	2%	50%
	1964	LW1	0.33	1.8704±0.0027	1.8791	0%	1.5868	3%	50%
	1965	EW1	0.33	1.7855±0.0026	1.7933	0%	1.7397	15%	50%
	1965	EW2	0.33	1.7857±0.0026	1.7914	0%	1.7397	11%	50%
	1965	LW1	0.33	1.7897±0.0026	1.7717	1%	1.7397	−56%	50%
Larch	1962	EW1	0.33	1.3329±0.0020	1.3819	−4%	1.2189	30%	50%
	1962	EW2	0.33	1.3928±0.0021	1.4027	−1%	1.2189	5%	50%
	1962	LW1	0.33	1.4306±0.0022	1.4063	2%	1.2189	−13%	50%
	1963	EW1	0.33	1.6962±0.0025	1.7599	−4%	1.3079	14%	50%
	1963	EW2	0.33	1.8115±0.0026	1.8931	−4%	1.3079	14%	50%
	1963	LW1	0.33	1.9001±0.0027	1.9437	−2%	1.3079	7%	50%
	1964	EW1	0.50	1.8992±0.0027	1.9011	0%	1.5868	1%	50%
	1964	LW1	0.50	1.9060±0.0026	1.8843	1%	1.5868	−7%	50%
	1965	EW1	0.33	1.7901±0.0026	1.7933	0%	1.7397	6%	50%
	1965	EW2	0.33	1.7902±0.0026	1.7914	0%	1.7397	2%	50%
	1965	LW1	0.33	1.7763±0.0026	1.7717	0%	1.7397	−14%	50%

The measured $F^{14}C$ can now be compared to the atmospheric $F^{14}C$ (direct assimilation). We assume here, that the atmosphere is well mixed within the region of study, an assumption supported by atmospheric measurements from Jungfraujoch (Levin et al. 2013), which compare well with the ones from Schauinsland (as long as there are no local sources of fossil CO_2). The difference we explain with a variable contribution (Table 2, *fraction NSC*) of a constant NSC storage pool that is refreshed every year at a specific exchange rate R (annual exchange rate of NSC storage pool, see also Table 2). $F^{14}C_{NSC}$ of the NSC storage pool for a specific year (y) is calculated by a recursive procedure from the previous year (y - *1*):

$$F^{14}C_{NSC}(y) = (1 - R) * F^{14}C_{NSC}(y - 1) + R * F^{14}C_{Atm}(y - 1)$$

where the replaced fraction R of the NSC storage pool has the same signature as the atmosphere ($F^{14}C_{Atm}$). The $F^{14}C_{NSC}$ is calculated for every year starting with the year 1951 (run-in of at least 10 years for comparison with measured data). For the best possible fit, we find that the exchange rate per year of the storage pool tends to be a bit higher for the oak and pine ($R = 70\%$) than for the spruce and larch ($R = 50\%$) from the elevated sites in the Lötschental. A low exchange rate will result in lower values than the atmosphere after 1963, while a high exchange rate will result in higher values. The exchange rate was thus fitted to give the best results for the years 1964 and 1965. In a last step, the *fraction NSC* for a specific year is estimated assuming the measured $F^{14}C$ of the cellulose ($F^{14}C_{Meas}$) is the sum of carbon directly assimilated from the atmosphere and of NSC from the storage pool, with their respective $F^{14}C$ signatures:

$$f(y) = \frac{F^{14}C_{Meas}(y) - F^{14}C_{Atm}(y)}{F^{14}C_{NSC}(y) - F^{14}C_{Atm}(y)}$$

Note that the results should only be considered significant, when the atmospheric $F^{14}C$ is significantly different from the $F^{14}C$ of the NSC storage pool, which is primarily the case for 1963 and 1964.

IMPLICATIONS AND DISCUSSION

The $F^{14}C$ measured in tree rings follows relatively closely the atmosphere during the time of growth. However, specific fractions as for example the EW fraction of the oak, deviate significantly from the atmosphere by up to 11%. The average deviation over the full annual rings is, however, much lower and only up to 3%.

A simple model was used to quantify the amount of stored carbon used by the tree to explain the observed discrepancies. The applied model, though neglecting naturally occurring variabilities (e.g., Carbone et al. 2013; Richardson et al. 2013), seems to predict relatively well the average use of NSC for specific trees.

Deciduous Trees

Unsurprisingly, because a newly formed earlywood is a prerequisite for the water supply during refoliation, the deciduous trees incorporate significant amounts of stored carbon from previous years in the EW, while the latewood is essentially built up from carbon of the current year (Michelot et al. 2012; Richardson et al. 2015). Especially the oak tree uses ca. 50% of the amount of stored carbon. This agrees well with the observation that a large portion of the EW is formed before budburst (and therefore before photosynthesis starts). Our results, however,

https://doi.org/10.1017/RDC.2024.38 Published online by Cambridge University Press

are not in agreement with observations done on similar $F^{14}C$ measurements on EW and LW of Danish and Swedish oak trees (Kudsk et al. 2018).

The stored carbon in oak trees seems to be of relatively young age because the $F^{14}C$ of the EW of 1965 is already increased compared with the atmosphere. Therefore, an average age for the carbon incorporated greater than 1–2 years is not indicated for the years analyzed (we estimated an average annual exchange rate of 70%). The deciduous conifer larch, being physiologically very different from the oak, also shows a detectable influence of stored carbon on the $F^{14}C$ of the first EW fraction. At 25% on average, the amount is only half as large as for the oak tree (where the EW fraction is also smaller). The storage pool in the larch seems to integrate over somewhat longer timescales, as the EW for 1965 the $F^{14}C$ was still not above the atmosphere, which would be expected for very short storage times.

Evergreen Conifer Trees

Even if the pine tree shows a significant influence on the $F^{14}C$ from the enhanced local anthropogenic CO_2 emission of fossil fuels, which we can correct for by an estimated fossil fuel contribution of 2%, the corrected $F^{14}C$-values in all tree-ring sections follow the atmosphere very closely. Therefore, no strong influence of stored carbon is visible, but a small contribution of stored carbon on the EW or the LW of less than 10% cannot be excluded, confirming data of Grootes et al. (1989) and Svarva et al. (2019) and physiological observations that evergreen conifers obtain their carbon for the wood structure mainly from current photosynthesis of the previous year's needles and less from reserve carbon (Michelot et al. 2012).

The spruce from the Lötschental shows again a clear contribution of stored carbon (up to 20%), but primarily in the LW, not in the EW. While the evergreen conifer tree spruce already assimilates CO_2 from the atmosphere in early spring, the amount is still expected to be small and thus a larger contribution of stored carbon was also expected on EW.

Implications for Tree Physiology

Several studies reported that earlywood growth, particularly in deciduous species, is supported by NSC pools from previous years as photosynthate production is still low. Gaudinski et al. (2009) reported that the age of these NSC was maximum of 1 year in white and chestnut oak whereas Muhr et al. (2016) found a mean age of the C of 3–5 years in sugar maple. Our results at the intra-annual level also indicate a substantial contribution of previous year reserves to earlywood. Such results also agree with previous studies that found a significant reduction of NSC pools (starch) at the beginning of the growing season in oak (Michelot et al. 2012). However, the values of the year 1965 can be a good example of how carbon from more than one previous year could be incorporated. Oak latewood sections showed a better fit with Vermunt measurements reinforcing the fact that growth will thus be mainly governed by recent assimilates. However, in oak the wood density of the earlywood (0.47 g/cm^3, SD ± 0.27 g/cm^3), which consists mainly of very large-lumen vessels, is clearly less than that of the latewood (0.74 g/cm^3, SD ± 0.15 g/cm^3) (Mayr et al. 2003), which consists mainly of very dense fiber cells and latewood vessels. The mass proportion of the earlywood in the total ring is therefore much lower than the mass proportion of the latewood. However, this depends to a considerable extent on the width of the annual rings. The width of the total annual rings shows clear fluctuations, caused by the site and weather-related growth conditions. However, the weather-related fluctuations are essentially only reflected in the latewood width, while the earlywood width shows very little year-to-year fluctuation.

https://doi.org/10.1017/RDC.2024.38 Published online by Cambridge University Press

Here, information from various approaches in plant synthesis is helpful, particularly in studying the age and seasonal use of actual versus stored NSCs in different species. There is a broad range of literature; here we refer to just two major publications and the references therein. Michelot et al. (2012) studied oak, pine and beech at lowlands east of Paris. They observed the beginning of oak growth 14 days before budburst, and a significant decrease of starch in this interval. For pine, the beginning of pine growth appeared coincident with budburst, and no change in NSC is seen. Richardson et al. (2015) studied ^{14}C of NSC on the outermost 20 rings of white pine and red oak in a temperate forest of the northeastern United States. The age of the NSC in the most recent five years was found to be less than 1 year, while older stem wood had NSC ages of more than 5 years. Grootes et al., 1989 found use of less than 15% of stored photosynthate, but a contribution of 13% to 28% CO_2 from decay of biological material, in a Sitka spruce at the Pacific coast of Washington.

Specific Implications for Annual ^{14}C Series on oak tree-rings

Since the absolute amount of earlywood of ring-porous oak wood is largely independent of the growing conditions, its relative proportion compared to the latewood has implications for high-resolution ^{14}C data measured on annual tree rings as demonstrated here. With narrow annual rings, the proportion of earlywood is significantly higher than with wide annual rings. Concerning the total annual ring, it is, therefore, to be expected that with narrow annual rings, i.e., with higher proportions of earlywood, the proportion of carbon from reserve materials in the cellulose will be higher than with wide annual rings, where the proportion of latewood with its higher density is significantly higher (Mayr et al. 2003).

However, before the bomb ^{14}C interval, the difference of $F^{14}C$ within 4 years or less in the atmosphere amounts to only a few permille, except for solar particle events (SPE), where it can be up to 12 permille in one year. Therefore, the uptake of ^{14}C in earlywood, especially of oak, must be considered in the period of rapid and strong fluctuations during the bomb tests and SPEs, but it is not statistically significant elsewhere. For most applications, total oak tree rings can therefore be used for producing high- resolution (even annual) ^{14}C time series.

CONCLUSIONS

Using the bomb ^{14}C signal (especially the years 1962–1965) generated during the nuclear bomb tests starting in the 1950s, our analyses were able to identify the contribution of NSCs from previous years before the growth year of the tree rings. In general, depending on the species mostly earlywood is affected. With regard to the suitability for high resolution (annual, resp. sub-annual) ^{14}C-series, we can summarize that there are clear differences between the different tree species we have investigated.

For the ring-porous deciduous oak, the cellulose of the earlywood shows a substantial contribution of stored carbohydrates from the previous year(s), whereas the latewood is formed exclusively from currently photosynthesized C. The earlywood of the deciduous conifer larch also shows a significant proportion of C from previous years, but to a much lesser extent than the oak, and the latewood follows the atmosphere closely. The evergreen pine, on the other hand, essentially does not seem to incorporate significant amounts of previous year(s) carbohydrates in either earlywood or latewood, even if there is some uncertainty here due to the increased fossil C input at that site. Finally, for spruce, a small proportion of reserve C is discernible in the earlywood, but the spruce also incorporates "older" stored carbohydrates into the latewood.

https://doi.org/10.1017/RDC.2024.38 Published online by Cambridge University Press

However, for pre-bomb years, earlier signals in earlywood are usually beyond the ^{14}C measurement error (1.5 to 2‰ at best), because of (1) the low contribution of earlywood to the total carbon mass of a ring, and (2) max. 15 permille/year change during SPEs, and 20 permille/60 years at strong solar minima. Hence, total tree-ring ^{14}C data are still useful for ^{14}C calibration using annual ^{14}C data of trees growing in a temperate oceanic climate. Only in special cases, such as comparisons of annual ^{14}C data sets between different regions/latitudes, the temporal differences of uptake of seasonal ^{14}C and incorporation of NSC in earlywood suggest focusing on latewood only, as documented here for oak and larch.

ACKNOWLEDGMENTS

This project was stimulated by the EC-MILLENNIUM project (EC grant 017008) and by the ESF EuroClimate project 'TREE-14' and completed with support of M.F. by the European Research Council under the European Union's Horizon 2020 Research and Innovation Program (grant agreement No. 803147 RESOLUTION awarded to S. Talamo, Bologna University).

We thank forest manager Lothar Bellert and the Community of Rust, Germany for helpful support on samples from 'Taubergiessen' nature reserve and Dr. Helmut Dalitz for samples from Hohenheim Gardens.

We thank Dr. Joachim Ingwersen, Institute of Soil Science and Land Evaluation, Dr. Tobias KD Weber, Land-Atmosphere Feedback Observatorium (LAFO) and Dr. Hans-Stefan Bauer, Institute of Physics and Meteorology, all from University of Hohenheim for helpful discussions and advice.

We would like to thank the Editor Steven Leavitt and the two reviewers for their valuable comments that improved the paper considerably.

SUPPLEMENTARY MATERIAL

To view supplementary material for this article, please visit https://doi.org/10.1017/RDC.2024.38

REFERENCES

Bayliss A, Marshall P, Dee MW, Friedrich M, Heaton TJ, Wacker L. 2020. IntCal20 tree rings: an archaeological swot analysis. Radiocarbon 62(4):1045–1078.

Boettger T, Friedrich M. 2009. A new serial pooling method of shifted tree-ring blocks to construct millennia long tree-ring isotope chronologies with annual resolution. Isotopes in Environmental and Health Studies 45(1):68–80.

Cain WF, Griffin S, Druffel-Rodriguez KC, Druffel ERM. 2018. Uptake of carbon for cellulose production in a white oak from western Oregon, USA. Radiocarbon 60(1):151–158.

Carbone MS, Czimczik CI, Keenan TF, Murakami PF, Pederson N, Schaberg PG, Xu X, Richardson AD. 2013. Age, allocation and availability of nonstructural carbon in mature red maple trees. Phytol 200:1145–1155.

Carrer M, Castagneri D, Prendin AL, Petit G, von Arx G. 2017. Retrospective analysis of wood anatomical traits reveals a recent extension in tree cambial activity in two high-elevation conifers. Front Plant Sci 8:737.

Chen Y, Rademacher T, Fonti P, Eckes-Shephard AH, LeMoine, Fonti MV, JM, Richardson AD, Friend AD. 2022. Inter-annual and inter-species tree growth explained by phenology of xylogenesis. New Phytologist 235:939–952.

Cuny HE, Fonti P, Rathgeber CBK, von Arx G, Peters R, Frank D. 2019. Couplings in cell differentiation kinetics mitigate air temperature influence on conifer wood anatomy. Plant Cell Environ 42:1222–1232.

Cuny HE, Rathgeber CBK, Frank D, Fonti P, Mäkinen H, Prislan P, Rossi S, del Castillo EM, Campelo F, Vavrčík H et al. 2015. Woody

biomass production lags stem-girth increase by over one month in coniferous forests. Nature Plants 1(11):15160.

Dox I, Mariën B, Zuccarini P, Marchand LJ, Prislan P, Gričar J, Flores O, Gehrmann F, Fonti P, Lange H et al. 2022. Wood growth phenology and its relationship with leaf phenology in deciduous forest trees of the temperate zone of Western Europe. Agricultural and Forest Meteorology 327:109229.

Epron et al. 2012. Pulse-labelling trees to study carbon allocation dynamics: a review of methods, current knowledge and future prospects. Tree Physiology 32:776–798.

Gaudinski JB, Torn MS, Riley WJ, Swanston C, Trumbore SE, Joslin JD, Majdi H, Dawson TE, Hanson PJ. 2009. Use of stored carbon reserves in growth of temperate tree roots and leaf buds: analyses using radiocarbon measurements and modeling. Global Change Biology 15:992–1014.

Gessler A, Treydte K. 2016. The fate and age of carbon – insights into the storage and remobilization dynamics in trees. The New Phytologist 209(4):1338–1340.

Grootes PM, Farwell GW, Schmidt FH, Leach DD. 1989. Rapid response of tree cellulose radiocarbon content to changes in atmospheric $^{14}CO_2$ concentration. Tellus 41B:134–148.

Hacke UG, Sperry JS. 2001. Functional and ecological xylem anatomy. Perspectives in Plant Ecology, Evolution and Systematics 4(2):97–115.

Helle G, Schleser GH. 2004. Beyond CO_2-fixation by Rubisco – an interpretation of $^{13}C/^{12}C$ variations in tree-rings from novel intra-seasonal studies on broad-leaf trees. Plant, Cell & Environment 27(3):367–380.

Holz I, Franzaring J, Böcker R, Fangmeier A. 2010. LUBW – Landesanstalt für Umwelt, Messungen und Naturschutz Baden-Württemberg (Ed.) 2010. Eintrittsdaten phänologischer Phasen und ihre Beziehung zu Wetter und Klima. ID Umweltbeobachtung U96-U51-N10. http://www.fachdokumente.lubw.baden-wuerttemberg.de/

Hua Q, Barbetti M, Rakowski AZ. 2013. Atmospheric radiocarbon for the period 1950–2010. Radiocarbon 55(4):2059–2072.

Kromer B, Lindauer S, Synal HA, Wacker L. 2013. MAMS—a new AMS facility at the Curt-Engelhorn-Centre for Achaeometry, Mannheim, Germany. Nuclear Instruments and Methods in Physics Research Section B: Beam Interactions with Materials and Atoms 294:11–13.

Kudsk SGK, Olsen J, Nielsen LN, Fogtmann-Schulz A, Knudsen MF, Karoff C. 2018. What Is the carbon origin of early-wood? Radiocarbon 60(5):1457–1464.

Levin I, Kromer B, Hammer S. 2013. Atmospheric delta (co2)-c-14 trend in western european background air from 2000 to 2012. Tellus Series B-Chemical and Physical Meteorology. 65.

Levin I, Kromer B, Schoch-Fischer H, Bruns M, Münnich M, Berdau D, Vogel JC, Münnich KO. 1985. 25 years of tropospheric 14C observations in central Europe. Radiocarbon 27:1–19.

Mayr C, Frenzel B, Friedrich M, Spurk M, Stichler W, Trimborn P. 2003. Stable carbon- and hydrogen-isotope ratios of subfossil oaks in southern Germany: methodology and application to a composite record for the Holocene. The Holocene 13(3):393–402.

McDonald L, Chivall D, Miles D, Bronk Ramsey C. 2019. Seasonal variations in the ^{14}C content of tree rings: Influences on radiocarbon calibration and single-year curve construction. Radiocarbon 61(1):185–194.

Michelot A, Simard S, Rathgeber C, Dufrêne E, Damesin C. 2012. Comparing the intra-annual wood formation of three European species (*Fagus sylvatica*, *Quercus petraea* and *Pinus sylvestris*) as related to leaf phenology and non-structural carbohydrate dynamics. Tree Physiology 32(8):1033–1045.

Moser L, Fonti P, Büntgen U, Esper J, Luterbacher J, Franzen J, Frank D. 2009. Timing and duration of European larch growing season along altitudinal gradients in the Swiss Alps. Tree Physiology 30(2):225–233.

Muhr J, Angert A, Negron-Juarez RI, Munoz WA, Kraemer G, Chambers JQ, Trumbore SE. 2013. Carbon dioxide emitted from live stems of tropical trees is several years old. Tree Physiology 33:743–752.

Muhr J, Messier C, Delagrange S, Trumbore S, Xu X, Hartmann H. 2016. How fresh is maple syrup? Sugar maple trees mobilize carbon stored several years previously during early springtime sap-ascent. New Phytologist 209(4):1410–1416.

Němec M, Wacker L, Hajdas I, Gäggeler H. 2010. Alternative methods for cellulose preparation for AMS measurement. Radiocarbon 52(3): 1358–1370.

Olsson IU, Possnert G. 1992. ^{14}C activity in different sections and chemical fractions of oak tree rings, AD 1938–1981. Radiocarbon 34(3):757–767.

Pérez-de-Lis G, Rathgeber CBK, Fernández-de-Uña L, Ponton S. 2022. Cutting tree-rings into time slices: how intra-annual dynamics of wood formation help decipher the space-for-time conversion. New Phytol 233:1520–1534.

Rathgeber C, Cuny H, Fonti P. 2016. Biological basis of wood formation: a crash course. Frontiers in Plant Sciences 7:734.

Rathgeber CBK, Pérez-de-Lis G, Fernández-de-Uña L, Fonti P, Rossi S, Treydte K, Gessler A, Deslauriers A, Fonti MV, Ponton S. 2022. Anatomical, developmental and physiological bases of tree-ring formation in relation to environmental factors. In: Siegwolf RTW, Brooks JR, Roden J, Saurer M, editors. Stable isotopes in tree-rings: inferring physiological, climatic and environmental

https://doi.org/10.1017/RDC.2024.38 Published online by Cambridge University Press

responses. Cham: Springer International Publishing. p. 61–99.

Reimer PJ, Austin WEN, Bard E, Bayliss A, Blackwell PG, Ramsey CB, Butzin M, Cheng H, Edwards RL, Friedrich M et al. 2020. The IntCal20 Northern Hemisphere radiocarbon age calibration curve (0–55 cal kbp). Radiocarbon 62(4):725–757.

Reimer PJ, Baillie MGL, Bard E, Bayliss A, Beck JW, Bertrand CJH, Blackwell PG, Buck CE, Burr GS, Cutler KB et al. 2004. Intcal04 terrestrial radiocarbon age calibration, 0–26 cal kyr bp. Radiocarbon 46(3):1029–1058.

Richardson AD, Carbone MS, Huggett BA, Furze ME, Czimczik CI, Walker JC, Xu X, Schaberg PG, Murakami P. 2015. Distribution and mixing of old and new nonstructural carbon in two temperate trees. New Phytologist 206(2): 590–597.

Richardson AD, Carbone MS, Keenan TF, Czimczik CI, Hollinger DY, Murakami P, Schaberg PG, Xu X. 2013. Seasonal dynamics and age of stemwood nonstructural carbohydrates in temperate forest trees. New Phytologist 197(3):850–861.

Rossi S, Anfodillo T, Čufar K, Cuny HE, Deslauriers A, Fonti P, Frank D, Gričar J, Gruber A, Huang J-G et al. 2016. Pattern of xylem phenology in conifers of cold ecosystems at the northern hemisphere. Global Change Biology 22(11):3804–3813.

Sookdeo A, Kromer B, Büntgen U, Friedrich M, Friedrich R, Helle G, Pauly M, Nievergelt D, Reinig F, Treydte K et al. 2020. Quality dating: a well-defined protocol implemented at ETH for high-precision ^{14}C-dates tested on Late Glacial wood. Radiocarbon 62(4):891–899.

Stuiver M, Kromer B, Becker B, Ferguson C. 1986. Radiocarbon age calibration back to 13,300 years BP and the ^{14}C age matching of the German oak and US bristlecone pine chronologies. Radiocarbon 28(2B):969–979.

Svarva H, Grootes P, Seiler M, Stene S, Thun T, Værnes E, Nadeau M-J. 2019. The 1953–1965 rise in Atmospheric bomb ^{14}C in central Norway. Radiocarbon 61(6):1765–1774.

Turney CSM, Palmer J, Maslin MA, Hogg A, Fogwill CJ, Southon J, Fenwick P, Helle G, Wilmshurst JM, McGlone M et al. 2018. Global peak in atmospheric radiocarbon provides a potential definition for the onset of the anthropocene epoch in 1965. Sci Rep-Uk 8(1):3293.

Wacker L, Bonani G, Friedrich M, Hajdas I, Kromer B, Nemec N, Ruff M, Suter M, Synal H-A, Vockenhuber C. 2010. MICADAS: routine and high-precision radiocarbon dating. Radiocarbon 52(2):252–262.

Wacker L, Nemec M, Bourquin J. 2010. A revolutionary graphitisation system: fully automated, compact and simple. Nucl Instrum Meth B 268:931–934.

Xu S, Cook GT, Cresswell AJ, Dunbar E, Freeman SPHT, Hastie H, Hou X, Jacobsson P, Naysmith P, Sanderson DCW. 2015. Radiocarbon concentration in modern tree-rings from Fukushima, Japan. Journal of Environmental Radioactivity 146:67–72.

https://doi.org/10.1017/RDC.2024.38 Published online by Cambridge University Press